Performance of inter-chip RF-interconnect using CPW, capacitive coupler and UWB transceiver

Sun, Mei; Zhang, Yue Ping

2005

Sun, M., & Zhang, Y.P. (2005). Performance of inter-chip RF-interconnect using CPW, capacitive coupler and UWB transceiver. IEEE Transactions on Microwave Theory and Techniques, 53(9), 2650-2655.

https://hdl.handle.net/10356/79996

https://doi.org/10.1109/TMTT.2005.854213

Performance of Inter-Chip RF-Interconnect Using CPW, Capacitive Coupler, and UWB Transceiver

M. Sun and Y. P. Zhang

***Abstract*—A novel inter-chip RF-interconnect system operating in the range of 22–29 GHz is described and analyzed in terms of system bit error rate (BER) performance. After characterizing the interconnect channel, plotting the transmitted and received ultra-wideband pulses, and estimating the switching noise power density by proposing a novel switching noise attack model, we finally get the results of the system performance. It is shown that the performance degrades with the interconnect distance and the switching noise attacker number. It is concluded that a high data rate at 3.33 Gb/s with a low $\mathrm{BER} < 10^{-5}$ over the entire chip of size 30×30 mm^2 is achievable with the radiated power density less than −41 dBm/MHz (or the average transmitted power less than −2.85 dBm).**

***Index Terms*—Bit error rate (BER), capacitive coupler, coplanar waveguide (CPW), inter-chip RF-interconnect (RFI), ultra-wideband (UWB) radio.**

I. Introduction

SEMICONDUCTOR technologies continuously scale down feature size to improve the speed of operation. Taking complementary metal–oxide semiconductor (CMOS) technology as an example, the minimum feature size of metal–oxide semiconductor (MOS) transistors has been reduced to 90 nm and the speed of operation has exceeded 100 GHz [1]. Such rapid scaling has two profound impacts. First, it enables a much higher degree of integration. Second, it implies a much greater challenge of the interconnect because the metal wire width and space are greatly reduced and fundamental material limits are approaching [2]. Revolutionary interconnect methods and techniques must be pursued to carry on the fast progress of future ultra large-scale integration (ULSI) technology. At this point, RF-interconnect (RFI) become possible with high-frequency silicon technologies and ever-increasing integrated-circuit (IC) size [3]–[6].

A novel RFI system concept is first proposed in [3]. Its structure is based on RF-transceiver and capacitive coupling over an impedance-matched transmission line, where RF signals are up-linked to the shared broadcasting medium, coplanar waveguide (CPW), or microstrip transmission line (MTL) via transmitting capacitive couplers, then down-linked via receiving capacitive couplers to fulfill the interconnect function. This RFI system structure overcomes the limits of conventional digital interface systems using the direct-coupled interconnect (DCI) and the capacitive coupled interconnect (CCI). It improves the signal-to-noise ratio and lowers the signal swing and output consumption while it increases the transmission data rate [4]. For this RFI system structure, it has demonstrated a maximum data rate of 2.2 Gb/s in 0.18-μm CMOS technology [4]. However, in [3]–[5], the transceivers of these previous RFI systems are all based on a traditional radio structure. As compared with conventional radios, the UWB radio is much simpler and there is no reference oscillator, frequency synthesizer, voltage-controlled oscillator, mixer, or power amplifier, which directly translates to smaller circuitry overhead and power consumption [7]. The concept of integration of an ultra-wideband (UWB) transceiver into a chip for an intra- and inter-chip wireless interconnect has been proposed in a novel configuration of wireless chip area networks (WCANs) as its physical layer [8]. In [9], the UWB radio is firstly proposed as the transceiver for the inter-chip RFI system using CPW and capacitive couplers. Based on this idea, a novel RFI system structure is proposed to offer an alternative solution for the chip-to-chip interconnect problem. It has the advantage of the small attenuation of the CPW and capacitive coupler channel, as well as the advantage of the UWB radio for short-range communication. In this paper, the performance of this RFI system will be analyzed in detail. The interconnect channel will be characterized and the transmitted and received UWB pulses will be plotted and, after that, a realistic switching noise attack model will be proposed to estimate the system SNR and evaluate the system bit error rate (BER) performance in terms of the different switching noise attack number.

II. System Structure and Performance Analysis

Fig. 1 shows the proposed inter-chip RFI system located inside a multichip module (MCM) package to fulfill the interconnect function between digital I/O A and B [9]. It uses UWB radios as transceivers, which comprises a pulse generator, a transmit/receive (T/R) switch, a low-noise amplifier (LNA), a matched filter, and a threshold circuit. In addition, this system features a unique channel, composed by capacitive couplers, and an off-chip, but in-package passive MTL or CPW as a shared broadcasting medium. The transmitted pulse is directly fed to the transmitting capacitive couplers. The information can be transmitted using pulse position modulation (PPM). The received pulse is passed through the matched filter. The original information is then recovered with an adjustable high-gain threshold circuit. The system operates at the 22–29-GHz UWB frequency band. The advantage of this higher band as opposed to the 3.1–10.6-GHz UWB band will be shown below.

Manuscript received December 17, 2004; revised March 17, 2005.

The authors are with the Integrated Systems Research Laboratory, School of Electrical and Electronic Engineering, Nanyang Technological University, Singapore 639798 (e-mail: SUNM0001@ntu.edu.sg; eypzhang@ntu.edu.sg).

Digital Object Identifier 10.1109/TMTT.2005.854213

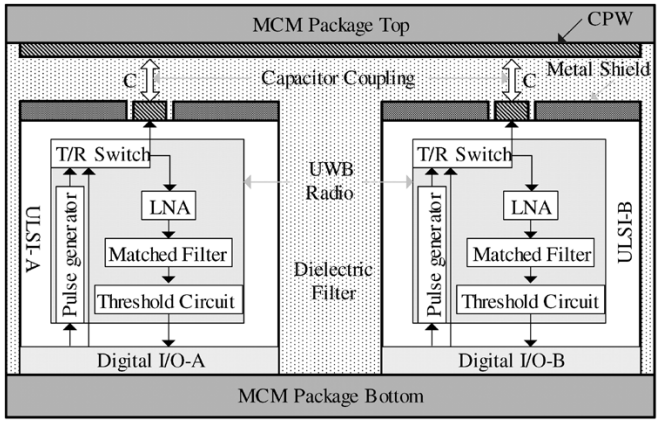

Fig. 1. Inter-chip RFI system architecture.

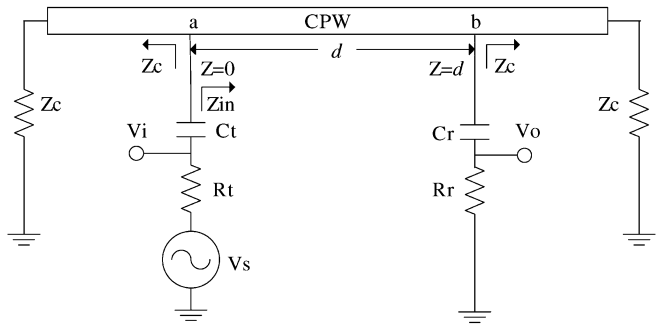

Fig. 2. Channel model: C_t is the transmitter's coupling capacitor, C_r is the receiver's coupling capacitor, R_t is the transmitter's output resistance, R_r is the receiver's input resistance, V_s is the source signal voltage, d is the distance between the transmitter and receiver, Z_{in} is the impedance looked into the CPW, V_i is the channel's input voltage, and V_o is the channel's output voltage.

A. Characterization of the Interconnect Channel

The channel comprises capacitive couplers and a shared CPW. The characteristic of this channel is first analyzed in [3] based on transmission-line theory with some approximation. Here, the channel's exact transfer function is derived as follows in (1) based on transmission-line theory using the channel model shown in Fig. 2 [9]:

$$H(f,d) = \frac{X_{C_t}+Z_c//Z_{\text{in}}}{(R_t+X_{C_t}+Z_c//Z_{\text{in}})} \cdot \frac{\left[(Z_{\text{in}}+Z_c)\exp(-\gamma d)+(Z_{\text{in}}-Z_c)\exp(\gamma d)\right]}{2(R_t+X_{C_t}+Z_{\text{in}})} \quad (1)$$

where

$$X_{C_t} = -j\frac{1}{\omega C_t}$$
$$X_{C_r} = -j\frac{1}{\omega C_r}$$
$$Z_{\text{in}} = Z_c\frac{(R_r+X_{C_r})//Z_c + Z_c\tanh\gamma d}{Z_c+(R_r+X_{C_r})//Z_c\tanh\gamma d}$$

$\gamma = \alpha + j\beta$ is the complex propagation constant of the CPW. Its real part α in nepers per meter represents the attenuation constant and its imaginary part β in radians per meter represents the phase constant. Based on the simulated frequency-dependant α and β values in [9], we examined the parameters' effect on the amplitude of transfer function H, as shown in Fig. 3(a)–(c). The parameters include the distance between the transmitter and receiver d, the coupler capacitance $C = C_t = C_r$, and the resistance $R = R_t = R_r$. Note that the value of coupler capacitance C and resistance R is the same for the transmitter and receiver because of our system's bidirectional communication nature. As expected, the amplitude of the transfer function shows the high-pass characteristic. In addition, Fig. 3(a) shows that the amplitude of H quickly decreases with distance. The longer distance has the larger attenuation. Fig. 3(b) shows that the coupler capacitance C has an important effect on the amplitude of H. The smaller capacitance has the larger channel attenuation. Based on this simulation, $C = 500$ fF is chosen for our system. Furthermore, it is found that output resistance R has a certain effect on the amplitude of H. R with a small value will cause the fluctuation of the amplitude of H in high frequency, as shown in Fig. 3(c). Based on this simulation, we choose $R = 5\,\text{k}\Omega$. The phase of the transfer function in terms of distance is also examined in Fig. 3(d). It shows the linear characteristic, and the longer distance has the larger delay. Based on the above observation, we conclude that the CPW and capacitive coupler channel can be regarded as a high-pass filter, which has a linear increased delay with interconnect length. This conclusion reconciles well with the measurement result in [10]. This high-pass characteristic of the channel can greatly reduce the switching noise coupling from the on-chip digital circuitry into the channel at the transmitter end, as illustrated in Fig. 4 [10]. It also explains why the higher UWB 22–29-GHz band is preferable to the lower band. However, for a realistic condition, switching noise will randomly couple to the CPW channel at any point. The more realistic switching noise model will be developed and the according average noise power spectral density (PSD) will be presented in Section II-C.

B. Transmitted and Received UWB Pulses

The PPM scheme is used in UWB radio. The designed UWB pulse was plotted in [9]. It has 0.25-ns time duration and 7-GHz bandwidth located from 22 to 29 GHz. The expression of transmitted UWB pulses using the PPM scheme was also presented in [9]. PPM delay is optimized as 0.02 ns. Appropriate frame width is chosen to realize the interconnect data rate $R_b = 3.33$ Gb/s. The peak amplitude of the transmitted pulse A is adjusted to change the transmitted energy per bit E_{tb}, e.g., when A is 0.03 V, we obtain the E_{tb} value of -131.4811 dB for 22–29-GHz bandwidth and the transmitted power density is less than -41 dBm/MHz.

Fig. 5(a) shows the transmitted data, transmitted pulses, and received pulses with normalized amplitude at $d = 20$ mm. It is found that the delay is serious. This can be explained by the channel transfer function H, which has linear increased delay with interconnect length. One method is developed in simulation to estimate the delay accurately. The result is shown in Fig. 6. As expected, the delay increases with distance. Using this estimated delay to compensate the received signal, we obtain the result, as shown in Fig. 5(b), which confirms the accuracy of delay estimation. Furthermore, the received signal suffers energy loss, as shown in Fig. 6, computed using a time-domain

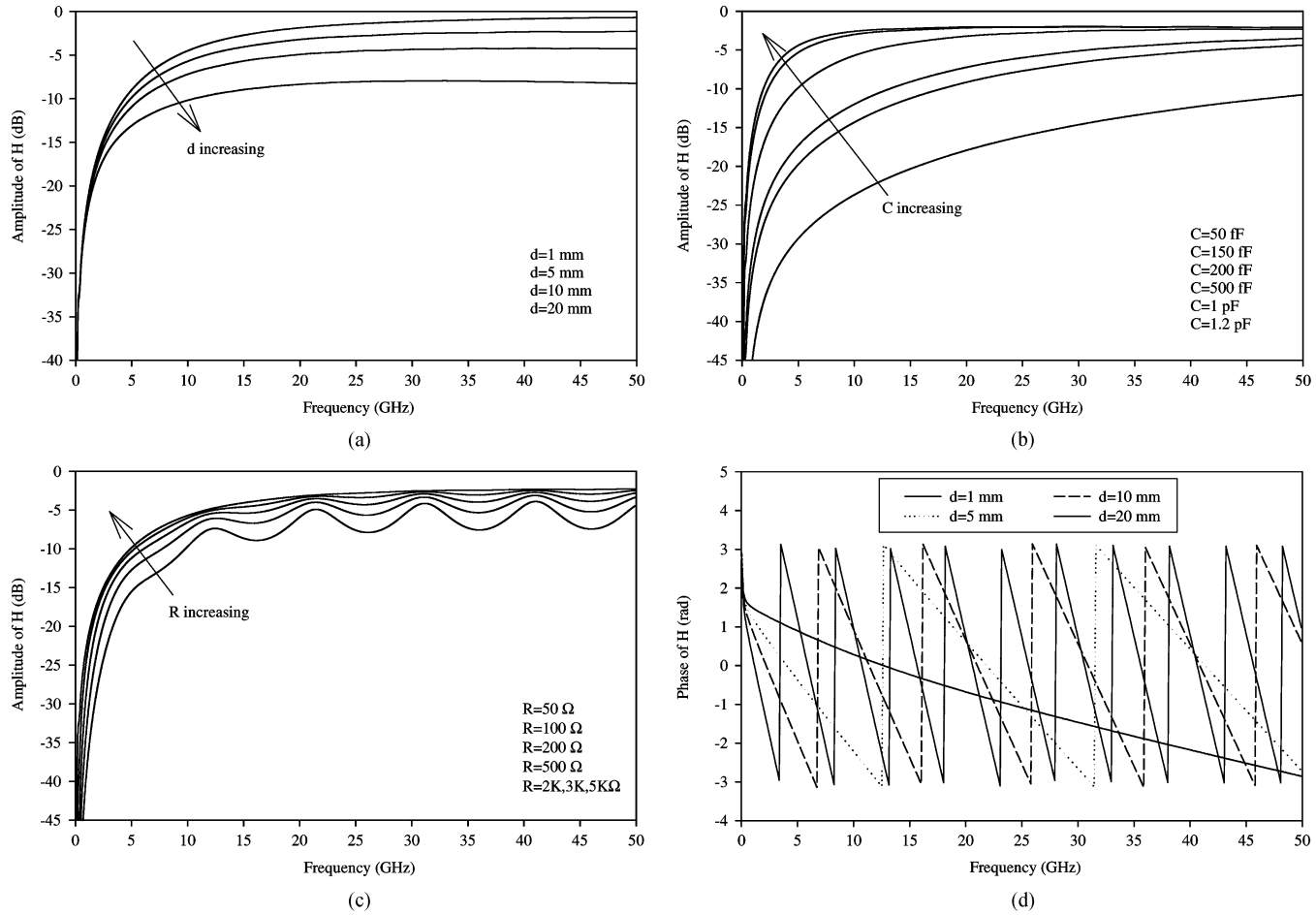

Fig. 3. Amplitude and phase of H versus frequency. (a) Effect of distance: $C = 500$ fF, $R = 5$ kΩ. (b) Effect of coupler capacitance: $d = 5$ mm, $R = 5$ kΩ. (c) Effect of resistance: $d = 5$ mm, $C = 500$ fF. (d) Effect of distance: $C = 500$ fF, $R = 5$ kΩ.

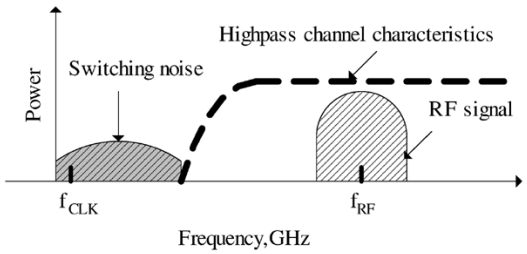

Fig. 4. Suppression of switching noise at the transmitter end in the RFI.

waveform of the signal after the channel. As expected, the energy loss Gloss increases with distance.

C. Switching Noise Attack Model

For our system that integrates both the analog radio front end and digital baseband processing circuits, the switching noise produced by the digital circuits may be significant and impact the receiver performance. Two types of switching noise coupling can be considered. The first type is the noise generated by the transistors in digital circuits injecting currents into the common substrate. Its effect on the system can be modeled by the capacitive coupling. The second is the noise capacitively coupled to the CPW in the same layer or from adjacent layers [11]. Therefore, the switching noise attack of both types can be modeled based on the capacitive coupling mechanism. Fig. 7 shows the attack by a switching noise source V_n on a victim CPW through capacitive coupling at the point p. The more realistic attacker waveform $V_n(t)$ as opposed to a piecewise-linear one is proposed in [11] based on the Markov chain and low-pass filter (LPF) model, as shown in Fig. 8. The switching noise activity is modeled by the Markov chain producing $d(t)$, whose PSD is shown as follows in (2), where a is the probability that a particular attacker switches and T is the shortest delay between state transition:

$$S_D\left(e^{j2\pi fT}\right) = \frac{a(1-a)}{1+(1-2a)^2-2(1-2a)\cos(2\pi fT)}. \quad (2)$$

The realistic attack noise waveform $V_n(t)$ is obtained by making $d(t)$ pass through a first-order LPF having a gain V and a time constant τ. Its PSD is then derived as

$$S_n(f,V) = S_D\left(e^{j2\pi fT}\right)\left|\frac{V^2}{(2\pi f\tau)^2+1}\right|. \quad (3)$$

For the switching noise attack model shown in Fig. 7, the transfer function $H_n(f,p)$ between V_0 and V_n can be exactly derived based on transmission-line theory according to the three cases $p < a, a \le p \le b$, and $b < p \le l$. The received noise

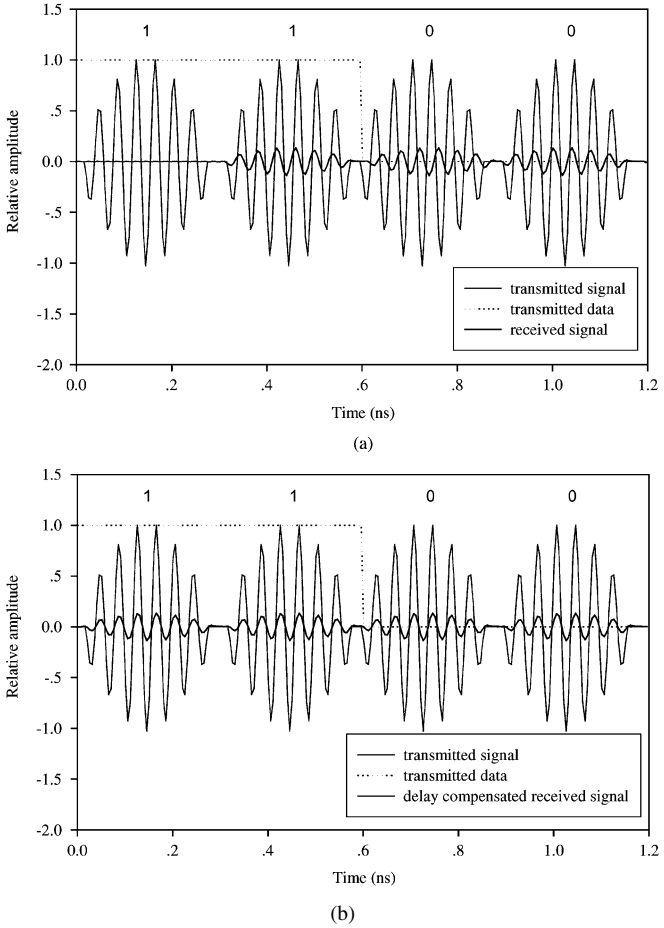

Fig. 5. Transmitted, received, and delay compensated received signal with normalized amplitude at $d = 20$ mm.

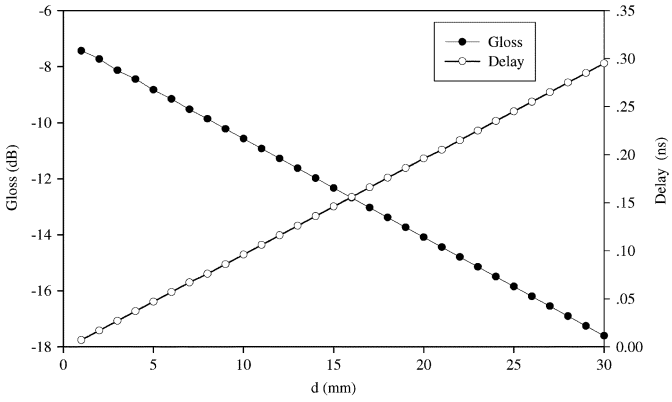

Fig. 6. Received signal's delay and energy loss versus distance.

PSD at V_0 contributed by the single noise attacker V_n is then obtained by

$$S_0(f) = S_n(f, V)|H_n(f, p)|^2. \tag{4}$$

It is assumed that the position of each attacker p is a random variable, which is uniformly distributed in the range of 0 to the CPW's length l. The gain V is also assumed to be a random variable having the uniform distribution in the range from 0 to 1. To consider the realistic case of many switching noise attackers to the victim CPW, the total PSD of the noise at V_0 is determined

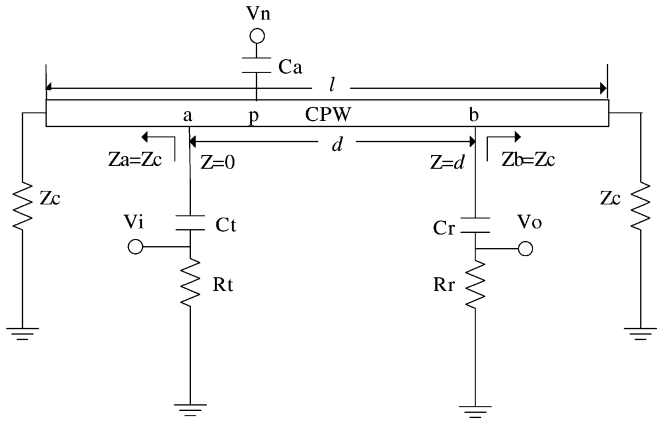

Fig. 7. Switching noise attack model.

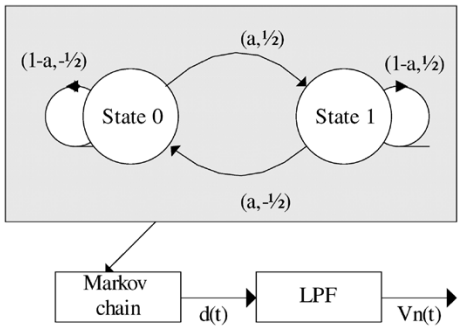

Fig. 8. Markov chain model for the switching activity of attackers.

by superposing the contribution of each individual attacker. In MATLAB, we simulated the average PSD at V_0 for the case of the number of attacker of 5, 10, and 15, respectively, which is calculated by

$$S_{0,\mathrm{av}}(f) = \frac{1}{N}\sum_{j=1}^{N}\sum_{i=1}^{5,10,15} S_n(f, V_{ij})|H_n(f, p_{ij})|^2 \tag{5}$$

where N is the total test number, j is the test index, and i represents the ith switching noise attacker. In every test, a noise source's coupling gain V_{ij} and coupling position p_{ij} is produced randomly according to their distribution. $H_n(f, p_{ij})$ is then calculated according to its position p_{ij}. The simulated $S_{0,\mathrm{av}}(f)$ at the attacker number of 5, 10, and 15, respectively, is shown in Fig. 9. As expected, the $S_{0,\mathrm{av}}(f)$ increases with the number of attacker. It is also worth noting that the $S_{0,\mathrm{av}}(f)$ has no dc component and is fairly flat in the frequency range of 22–29 GHz. Its average value in this frequency range S_0 will be used to estimate the average bit SNR at the receiver end in Section II-D. The exact transfer function and realistic switching noise attack model presented here makes it possible to realistically model the switching noise PSD on the victim line, which will provide important information to evaluate our system's performance.

D. BER Performance

For an inter-chip interconnect within a package, the signal is only contaminated by thermal noise and switching noise. The expression of the thermal noise PSD N_0 has been presented in [9] based on the receiver noise figure F_r. It is shown that F_r

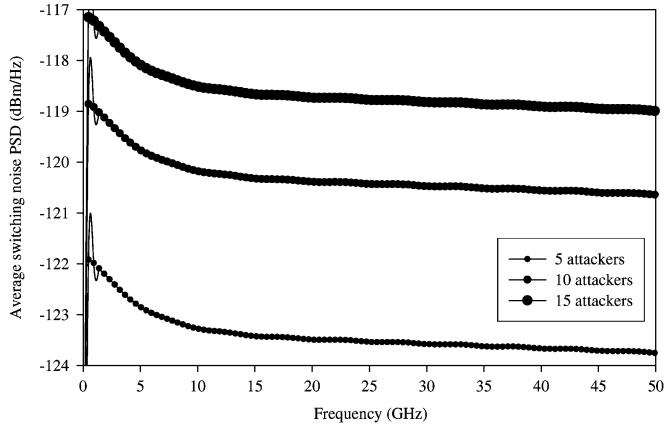

Fig. 9. Average switching noise PSD versus frequency.

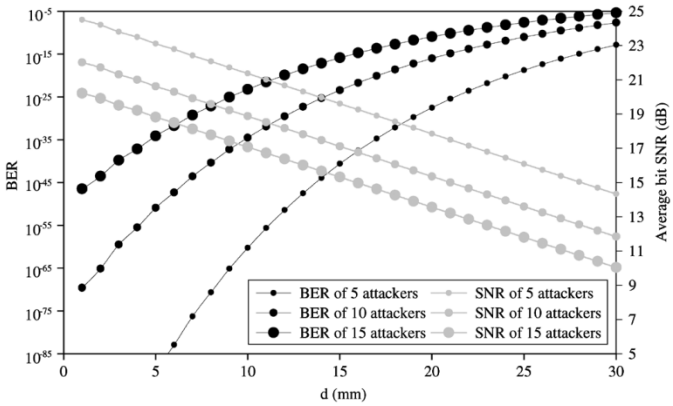

Fig. 10. Average bit SNR and BER versus distance for a different attacker number.

is 6.6 dB in the lower band and 8.6 dB in the upper band for a CMOS UWB radio operating from 3.1 to 10.6 GHz [12], [13]. Thus, here, F_r can be reasonably assumed to be 15 dB. The simulated average switching noise PSD was obtained in Section II-C as S_0. The average bit SNR at the receiver end is then shown as follows:

$$\Gamma_b = \frac{E_{rb}}{N_0 + S_0} \tag{6}$$

where E_{rb} is the received average energy per bit calculated using the expression presented in [9] based on the gain of the receiver G_r and the implementation margin G_m.

The BER of our system using PPM modulation is then obtained as a Q-function [9]

$$P_b = Q(\sqrt{(1-\rho)\cdot\Gamma_b}) \tag{7}$$

$$\rho = \frac{\int_0^{T_f} g'(t)g'(t-\delta)\,dt}{\int_0^{T_f} g'^2(t)\,dt} \tag{8}$$

where $g'(t)$ is the received pulse corresponding to our designed pulse $g(t)$ without delay and the PPM delay δ is optimized as 0.02 ns to obtain the best BER performance.

The average bit SNR Γ_b and BER versus distance for the different attacker number are shown in Fig. 10. The parameters used in simulation are $G_m = 4$ dB, $G_r = 15$ dB, and $F_r = 15$ dB and the peak amplitude of the transmitted pulse A is adjusted to 0.03 V. As expected, Γ_b decreases with distance and the attacker number. The BER increases with distance and the attacker number. It is concluded that a high interconnect data rate at 3.33 Gb/s with a low $\mathrm{BER} < 10^{-5}$ over the entire chip of size 30×30 mm^2 is achievable with the radiated power density less than -41 dBm/MHz (or the average transmitted power less than -2.85 dBm).

III. Conclusion

A novel inter-chip RFI system operating in the range of 22–29 GHz has been described and analyzed in terms of system BER performance. This system features a channel comprised by the CPW and capacitive couplers. It also features an UWB radio as the transceiver. For this system, the transmitted UWB pulse is designed and the transfer function of the interconnect channel is derived; after that, a realistic switching noise attack model is proposed to estimate the system SNR and evaluate the system BER performance in terms of the different attack number. As expected, the BER increases with distance and the attacker number. It is concluded that a high data rate at 3.33 Gb/s with a low $\mathrm{BER} < 10^{-5}$ over the entire chip of size 30×30 mm^2 is achievable with the radiated power density less than -41 dBm/MHz (or the average transmitted power less than -2.85 dBm).

References

[1] *International Technology Roadmap for Semiconductors (ITRS)*, 2002 Update, SIA.
[2] R. H. Havemann and J. A. Hutchby, "High-performance interconnects: An integration overview," *Proc. IEEE*, vol. 89, no. 5, pp. 586–601, May 2001.
[3] M. F. Chang, V. P. Roychowdhury, L. Zhang, S. Hyunchol, and Y. X. Qian, "RF/wireless interconnect for inter- and intra-chip communications," *Proc. IEEE*, vol. 89, no. 4, pp. 456–466, Apr. 2001.
[4] H. Shin, Z. Xu, and M. F. Chang, "RF-interconnect for multi-Gb/s digital interface based on 10 GHz RF-modulation in 0.18 μm CMOS," *IEEE MTT-S Int. Microwave Symp. Dig.*, vol. 1, pp. 477–480, Jun. 2002.
[5] H. Shin and M. F. Chang, "1.1 Gbit/s RF-interconnect based on 10 GHz RF-modulation in 0.18 μm CMOS," *Electron. Lett.*, vol. 38, no. 2, pp. 71–72, Jan. 2002.
[6] Y. P. Zhang, "Bit-error-rate performance of intra-chip wireless interconnect systems," *IEEE Commun. Lett.*, vol. 8, no. 1, pp. 39–41, Jan. 2004.
[7] J. Foerster, E. Green, S. Somayazulu, and D. Leeper, "Ultra-wideband technology for short- or medium-range wireless communications," *Intel Technol. J. Q2*, pp. 1–11, 2001.
[8] Y. P. Zhang, "Wireless chip area network: A new paradigm for antennas, RF(MM)IC's, and communications," presented at the Asia–Pacific Microwave Conf., 2004.
[9] M. Sun and Y. P. Zhang, "Inter-chip RF-interconnect using CPW, capacitive coupler and UWB transceiver," presented at the Asia–Pacific Microwave Conf., 2004.
[10] H. Shin, Z. Xu, K. Miyashiro, and M. F. Chang, "Estimation of signal-to-noise ratio improvement in RF-interconnect," *Electron. Lett.*, vol. 38, no. 25, pp. 1666–1667, Dec. 2002.
[11] M. Saint-Laurent, Z. Ajmal, M. Swaminathan, and J. D. Meindl, "A model for interlevel coupling noise in multilevel interconnect structures," in *Interconnect Technol. Conf.*, vol. 4–6, Jun. 2001, pp. 110–112.
[12] *IEEE Standard 802.15-03/139r5*, 2003.
[13] *IEEE Standard 802.15-03/334r3*, 2003.

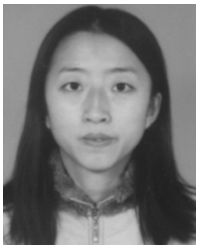

M. Sun was born in Gansu, China, in 1980. She received the B.S. degree in electrical and information engineering from the Hunan University, Hunan, China, in 2000, the M.S. degree in electronic engineering from the Beijing Institute of Technology, Beijing, China, in 2003, and is currently working toward the Ph.D. degree in electrical and electronic engineering at Nanyang Technological University, Singapore.

Her research interests include intra- and inter-chip RF wireless communication system simulation and implementation and integrated antenna design for wireless communication.

Y. P. Zhang received the B.E. degree from Taiyuan Polytechnic Institute, Shanxi, China, in 1982, the M.E. degree from and the Shanxi Mining Institute of Taiyuan University of Technology, Shanxi, China, in 1987, and the Ph.D. degree from the Chinese University of Hong Kong, Hong Kong, in 1995, all in electronic engineering.

From 1982 to 1984, he was with the Shanxi Electronic Industry Bureau. From 1990 to 1992, he was with the University of Liverpool, Liverpool, U.K. From 1996 to 1997, he was with the City University of Hong Kong. From 1987 to 1990, he was with the Shanxi Mining Institute. From 1997 to 1998, he was with the University of Hong Kong. In 1996, he became a Full Professor with the Taiyuan University of Technology. He is currently an Associate Professor with the School of Electrical and Electronic Engineering, Nanyang Technological University, Singapore. He currently guides a research group with the Integrated Systems Research Laboratory, School of Electrical and Electronic Engineering, Nanyang Technological University, to develop radio technologies for inter- and intra-chip wireless interconnection, communications, and networking. He has been involved in the areas of propagation of radio waves, characterization of radio channels, miniaturization of antennas, and implementation of wireless communications systems. He is listed in Marquis ' *Who's Who in Science and Engineering* and Cambridge University Press's *IBC 2000 Outstanding Scientists of the 21st Century*. He serves on the Editorial Board of the *International Journal of RF and Microwave Computer-Aided Engineering* and was a Guest Editor of the journal for the "Special Issue on RF and Microwave Subsystem Modules for Wireless Communications."

Prof. Zhang was the recipient of the 1990 Sino-British Technical Collaboration Award for his contribution to the advancement of subsurface radio science and technology. He was also the recipient of the 2000 Best Paper Award presented at the Second International Symposium on Communication Systems, Networks and Digital Signal Processing, Bournemouth, U.K.